ACS APPLIED MATERIALS & INTERFACES

Research Article

www.acsami.org

Polyelectrolyte Interlayer for Ultra-Sensitive Organic Transistor Humidity Sensors

Yeong Don Park,[†,#] Boseok Kang,[‡,#] Ho Sun Lim,[§] Kilwon Cho,[‡] Moon Sung Kang,*[,∥] and Jeong Ho Cho*[,⊥]

[†]Department of Energy and Chemical Engineering, Incheon National University, Incheon, 406-772, Korea

[‡]Department of Chemical Engineering, Pohang University of Science and Technology, Pohang, 790-784, Korea

[§]Electronic Materials and Device Research Center, Korea Electronics Technology Institute, Gyeonggi-do, 463-816, Korea

[∥]Department of Chemical Engineering, Soongsil University, Seoul, 156-743, Korea

[⊥]SKKU Advanced Institute of Nanotechnology (SAINT) and Center for Human Interface Nano Technology (HINT), School of Chemical Engineering, Sungkyunkwan University, Suwon, 440-476, Korea

Supporting Information

ABSTRACT: We demonstrate low-voltage, flexible, transparent pentacene humidity sensors with ultrahigh sensitivity, good reliability, and fast response/recovery behavior. The excellent performances of these devices are derived from an inserted polyelectrolyte (poly[2-(methacryloyloxy)-ethyltrimethylammonium chloride-*co*-3-(trimethoxysilyl)propyl methacrylate] (poly(METAC-*co*-TSPM)) interlayer, which releases free Cl^- ions in the electrolyte dielectric layer under humid conditions and boosts the electrical current in the transistor channel. This has led to extreme device sensitivity, such that electrical signal variations exceeding 7 orders of magnitude have been achieved in response to a 15% change in the relative humidity level. The new sensors exhibit a fast responsivity and a stable performance toward changes in humidity levels. Furthermore, the humidity sensors, mounted on flexible substrates, provided low voltage (<5 V) operation while preserving the unique ultrasensitivity and fast responsivity of these devices. We believe that the strategy of utilizing the enhanced ion motion in an inserted polyelectrolyte layer of an OFET structure can potentially improve sensor technologies beyond humidity-responsive systems.

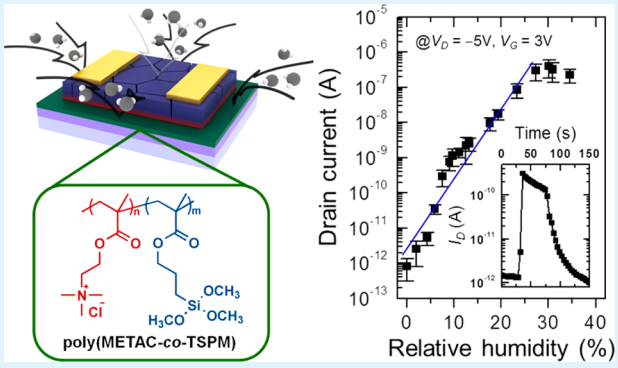

KEYWORDS: *polyelectrolyte interlayer, flexible humidity sensor, poly(METAC-co-TSPM), ultrasensitivity, fast response, organic transistor*

INTRODUCTION

Flexible electronics applications have attracted much interest over the last few decades.[1−5] In addition to transistors, electroluminescence devices, and energy conversion/storage devices,[6−10] the development of flexible sensors is also important for the future of flexible electronics.[11] In particular, humidity sensors, classical sensors widely used in industrial processes, are expected to significantly impact the biomedical field, agriculture, and daily life, if they can exhibit mechanical flexibility.[12] Of course, such sensors should be fabricated using flexible materials and should be highly sensitive, responsive, and stable under humid conditions. Accordingly, a variety of signal transduction techniques have been explored for monitoring changes in (i) the capacitance/resistance/impedance of a polymer/carbon/inorganic nanostructure[13−20] or (ii) the plasmonic resonance of a Au nanorod-embedded polymer nanofibers.[21]

Among various techniques developed, organic field-effect transistor (OFET) platforms have emerged as promising flexible sensor technologies because they are susceptible to chemical/physical stimuli.[22] Sensors based on transistors should ideally have a high sensitivity because such devices combine sensing and signal amplification capabilities such that a small change in the electrical environment, as induced by an analyte, leads to a pronounced change in the electrical current.[23] Low-cost, high-throughput sensing and feasible integration with flexible substrates are additional advantages of OFET-based sensors.[24,25] The sensing characteristics of OFET-based humidity sensors reported thus far, however, need improvement before they may be implemented in practice. In a typical transistor-based sensor, analytes must arrive at the environment/semiconductor interface, diffuse into the bulk of the semiconductor, and finally reach the semiconductor/gate-dielectric interface to influence the electrical signal measur-

Received: May 29, 2013
Accepted: August 12, 2013
Published: August 12, 2013

Scheme 1. (a) Schematic Diagram Showing a Typical OFET Humidity Sensor, (b) Schematic Diagram Showing a New OFET Sensor Containing an Inserted Humidity-Responsive Gate Dielectric Layer, and (c) Reaction Scheme Used to Synthesize Poly(METAC-*co*-TSPM)

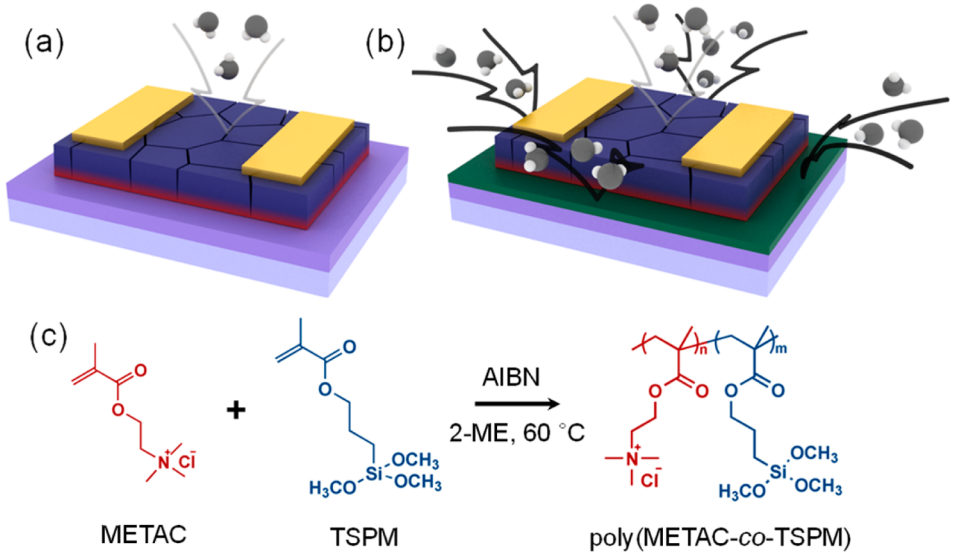

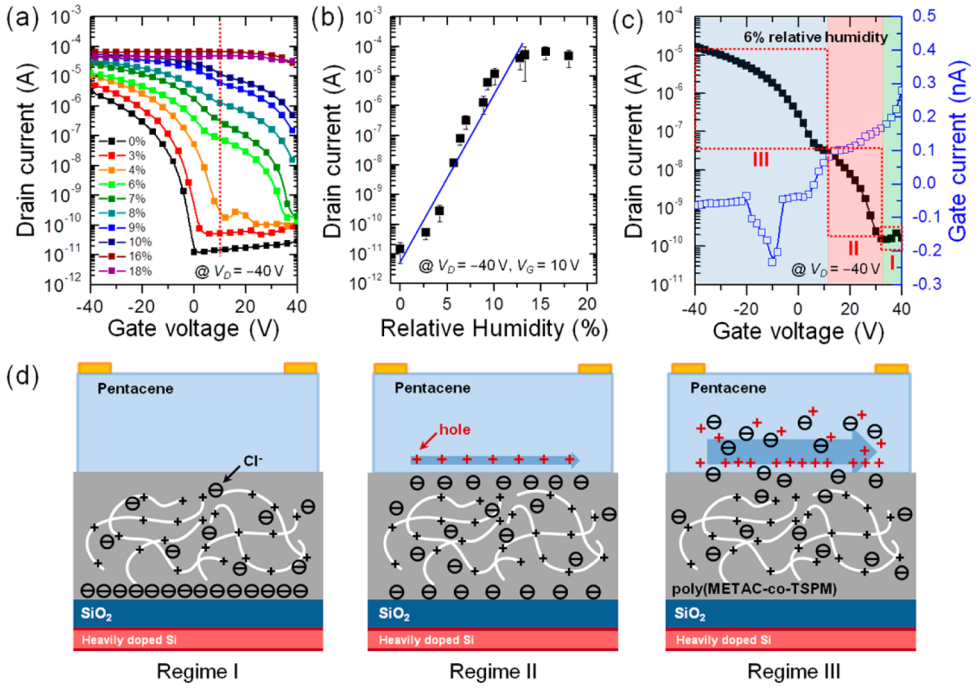

Figure 1. (a) Transfer characteristics at various humidity levels (V_D = −40 V). (b) Plot of I_D at V_G = 10 V and V_D = −40 V as a function of the humidity level. (c) A representative transfer characteristic plotted with I_G (V_D = −40 V). (d) Schematic diagrams of the proposed working principles under different V_G regimes.

ably.[24,25] Reaching of the analytes at the semiconductor/gate-dielectric interface is important because the majority of electrical charge transport in an OFET takes place at this interface (shown in red in Scheme 1a).[26] Unless analyte diffusion through the semiconductor is highly efficient, however, this type of sensor inevitably suffers from a slow response and a low sensitivity.

We attempted to address this issue by developing an OFET-type humidity sensor based on a new operating principle, in which a humidity-responsive polyelectrolyte layer, poly[2-(methacryloyloxy)ethyltrimethylammonium chloride-*co*-3-(trimethoxysilyl)propyl methacrylate] (poly(METAC-*co*-TSPM), inserted between organic semiconductor and gate dielectric layers, is directly exposed to humid environment (shown in green in Scheme 1b). The responsive behavior of the new sensor originates from the enhanced migration of mobile ions within the polyelectrolyte upon the absorption of moisture. This has led to extreme device sensitivity, such that electrical signal variations exceeding 7 orders of magnitude have been achieved in response to only a 15% change in the relative humidity level. Also, the new sensors exhibit a fast responsivity and a stable performance toward changes in humidity levels.

Furthermore, the humidity sensors, mounted on flexible substrates, provided low voltage (<5 V) operation while preserving the unique ultrasensitivity and fast responsivity of these devices. We believe that the strategy of utilizing the enhanced ion motion in an inserted polyelectrolyte layer of an OFET structure can potentially improve sensor technologies beyond humidity-responsive systems.

EXPERIMENTAL SECTION

Poly(METAC-*co*-TSPM) was synthesized through conventional free radical copolymerization techniques (Scheme 1c).[27,28] All reagents and starting materials were purchased from Aldrich Chemical Inc. METAC, the humidity-responsive unit, was purified on an alumina column after evaporating water. TSPM, a sol−gel precursor to form a polymer network through inter-/intra-polymer cross-linking and to assist in anchoring the polyelectrolytes onto the oxide substrates,[29] was used without further purification. α,α'-Azobisisobutyronitrile (AIBN) was recrystallized using methanol. A mixture of METAC (16.56 g, 80 mmol), TSPM (4.96 g, 20 mmol), and AIBN (0.16 g, 0.1 mmol) was dissolved in anhydrous 2-methoxyethanol (150 g) and degassed three times using the freeze−thaw method. The sealed reaction mixture was then heated and maintained at 60 °C for 12 h. The resulting polymerized mixture was isolated after precipitation (twice using THF), vacuum filtration, and freeze-drying. The molar composition of the resulting copolymers was 4:1 (METAC:TSPM).[29]

For sensor fabrications, poly(METAC-*co*-TSPM) was dissolved in methanol and spin-coated (3000 rpm, 60 s) onto a highly doped *n*-Si wafer with a 300 nm thick thermally grown oxide layer. The film was annealed at 80 °C for 12 h under humid conditions (relative humidity of 60%) to yield ∼30 nm thick polyelectrolyte layer. The thermal annealing induced cross-linking of the polymers. The resulting films were not dissolvable to the original solvent (methanol) employed for spin-coating, confirming the cross-linking of the polymers. Next, pentacene (50 nm) was thermally deposited onto the polyelectrolyte layer at a substrate temperature of 25 °C. Thermally evaporated source/drain gold electrodes were patterned using a shadow mask. The channel length and width were 150 and 1500 μm, respectively. A separate set of reference pentacene OFET devices devoid of the polyelectrolyte layer was also fabricated on SiO_2/Si substrates. In addition, flexible sensors were prepared by spin-coating the polyelectrolyte layer onto an Al_2O_3 (100 nm)/ITO/PET substrate. A photoresist was then deposited and removed to introduce roughness into the surface prior to pentacene deposition. Finally, graphene electrodes were transferred according to procedures reported previously.[8]

The electrical properties of the sensors were characterized at room temperature in a dark environment under a N_2 atmosphere using a Keithley 2636A instrument. Gaseous mixtures of dry and wet N_2 were introduced into the test chamber. The composition of the mixtures (thereby the relative humidity of the delivered gas) was controlled using mass flow controllers connected to a dry and wet N_2 tank. The relative humidity values were measured using a calibrated hygrometer (Testo) with an accuracy of ±0.1% relative humidity value.

RESULTS AND DISCUSSION

Figure 1a shows the transfer characteristics (the drain current (I_D) versus the gate voltage (V_G)) at a fixed drain voltage (V_D) of −40 V and at various relative humidity levels ranging from 0 to 18% for pentacene FET sensors prepared with an inserted polyelectrolyte layer. At a relative humidity of 0%, the devices exhibited typical $I-V$ characteristics of pentacene FETs with a turn-on voltage near 0 V such that I_D increased with increasing negative V_G. Because Cl^- ions bound tightly to the N^+ group in the polyelectrolyte backbone in the absence of moisture, no electrochemical processes were likely to occur.[27] Therefore, at zero humidity, the device operation was based on the electrostatic nature of the two insulating layers (SiO_2 and polyelectrolyte layers) connected in series to form the gate dielectric layer of a transistor.

As the relative humidity level increased, the overall current level was enhanced and the turn-on voltage shifted toward more positive values. The current level increased to a greater extent under positive V_G values than under negative V_G values. Figure 1b shows the average current levels of the transfer characteristics at V_G = 10 V for three different samples as a function of the relative humidity level. The error bar indicates the standard deviation of electrical currents obtained from the three different devices. Within the humidity range examined, the current level was amplified from tens of pA up to hundreds of μA (7 orders of magnitude!), demonstrating the extreme sensitivity of these sensors. Such a dramatic change in the output signal has not been achieved previously. To the best of our knowledge, ∼3 orders of magnitude change in the output signal in response to humidity is the maximum signal variation achievable from different types of humidity sensors available.[16−18,24,25,30] In addition, we note that the drain current of the sensors was saturated above a relative humidity level of ∼15%. The origin of the current saturation is discussed below. Before the saturation occurred, the log of the drain current exhibited a linear relation with the humidity level (the blue line in Figure 1b).

For comparison, the reference FETs prepared without an inserted polyelectrolyte layer displayed completely different responses to the presence of moisture. Supporting Information Figure S1 shows the transfer characteristics of the reference devices at relative humidity levels of 0 and 30% (which is an even more humid condition than a relative humidity level of 18% for comparison). The off-current levels of the reference samples at positive V_G values remained nearly invariant, whereas the levels at negative V_G values tended to decrease as the humidity level increased. In fact, the current through a pentacene film has been reported to degrade as the detrimental interactions between holes and water molecules are enhanced.[24,25] In addition, the reference devices displayed a shift in the turn-on voltage toward negative values rather than positive values (as was observed from the sensor with the interlayer). Overall, neither the current level variances nor the turn-on voltage shifts were as dramatic as those observed in the devices including an inserted polyelectrolyte layer.

Alternativley, resistor-type humidity sensors comprising only the poly(METAC-*co*-TSPM) between electrodes were fabricated, and their response to humidity was examined. These sensors did exhibit enhancement in the current signal as the relative humidity level was increased (Supporting Information Figure S2), confirming the moisture sensitive conductivity of the polyelectrolyte layer. However, their current amplification (an order of magnitude) was significantly smaller than the current variation of the corresponding OFET sensors with the interlayer at the same relative humidity level (7 orders of magnitude). These results indicate that enhanced conductivity of the poly(METAC-*co*-TSPM) interlayer cannot be the main origin of the extreme sensitivity of these new devices.

Instead, we consider that the key feature of this sensing system originated from the presence of Cl^- ions released from the polyelectrolyte backbone upon exposure to moisture. The working principle and the shape of the transfer characteristics of these new sensors are discussed in view of the trajectories of these freely released Cl^- ions. In the presence of humidity, the transfer characteristics contained an inflection point within the ON state operation regime. For example, Figure 1c displays the

transfer curve obtained at a relative humidity level of 6%. The inflection point and the turn on voltage marked the boundaries between three distinct voltage regimes: Regimes I, II, and III, starting from the regime characterized by the most positive gate voltages. The presence of the inflection point suggests that conduction through these devices under humid conditions was governed by a different mechanism under different gate voltage ranges.

In Regime I, where the highest positive V_G values were applied, most of the freely released Cl^- ions migrated to the SiO_2/polyelectrolyte interface due to the presence of a strong positive gate field (the left panel in Figure 1c). Consequently, Cl^- ions, although released from the polyelectrolyte backbone, did not significantly influence hole transport at the pentacene/electrolyte interface. The transistor, therefore, remained in the OFF state over this operation regime. We note that the OFF state current level did increase with the humidity level; however, this effect could be simply ascribed to enhanced current leakage through an electrolyte system in the presence of water molecules.[25,31]

Smaller but positive V_G values were applied in Regime II, and a fraction of the Cl^- ions were capable of escaping from the SiO_2/polyelectrolyte interface under the weaker gate field. The escaped Cl^- ions were then distributed over the polyelectrolyte layer. The ions near the pentacene/electrolyte interface contributed to hole formation in the transport channel or to electrochemical doping of the pentacene (the mid panel in Figure 1c). The turn-on voltage of the device consequently shifted toward positive values. It should be noted that the observation of a positive turn-on voltage from a *p*-type transistor indicates hole doping.[31−33] As V_G decreased, a higher number of Cl^- ions contributed to hole accumulation at the pentacene/polyelectrolyte interface and, therefore, the current level was increased. At higher humidity levels, more Cl^- ions were released from the backbone, resulting in a higher level of Cl^- ion doping of the pentacene and a more positive shift in the turn-on voltage.

Upon application of a negative V_G value (Regime III), I_D increased as V_G became more negative. In this V_G regime, the freely released Cl^- ions were not attracted to the SiO_2/polyelectrolyte interface; rather, they were pushed to the pentacene/polyelectrolyte interface or even into the pentacene films through grain boundaries. The diffusion of Cl^- ions into the pentacene film abruptly enhanced the doping process, yielding a sudden increase in the current level at which the inflection point occurred in the transfer characteristic. Consistent results were observed in the gate current (I_G) versus the gate voltage curves obtained simultaneously during the I_D−V_G measurements (the blue curve in Figure 1c), such that the magnitude of I_G increased suddenly upon entering Regime III. The area under the I_G−V_G curve is proportional to the induced charge density in the semiconductor channel; therefore, the abrupt change in the shape of the I_G−V_G curve indicated the appearance of an additional driving force for hole formation in the pentacene channel.[5,34−36] This force was thought to originate from the negative gate field that herded the released Cl^- ions toward the pentacene/polyelectrolyte interface. A spike in the I_G−V_G curve was observed at higher negative V_G values, indicating that perhaps charge transfer (or a redox reaction) took place between the electrolyte and the semiconductor layers.[34] Although the precise origin of this peak remains unclear, it may be attributed to the reduction of Cl_3^- ions present in equilibrium with the Cl^- ions in an aqueous environment,[37] which facilitates oxidization/hole-doping of pentacene film.

The working principle of the device based chlorine ion doping of pentacene can favorably explains the saturated drain current signal at high humidity levels (above 15% in Figure 1b). Considering the finite capability of pentacene films to contain chlorine ions, the maximum efficacy of chlorine ion doping should be finite. Beyond a critical concentration, therefore, not all the released chlorine ions would contribute to inducing charges in the pentacene layer, and thereby the enhancement in the current level of the sensors in response to humidity would be saturated. The saturation in the current level is indeed observed in Figure 1b.

Achieving reliable and prompt sensor responses is an important requirement of high-performance sensors. We tested the device response to multiple instances of exposure to humid conditions. Figure 2a shows the transfer characteristics of

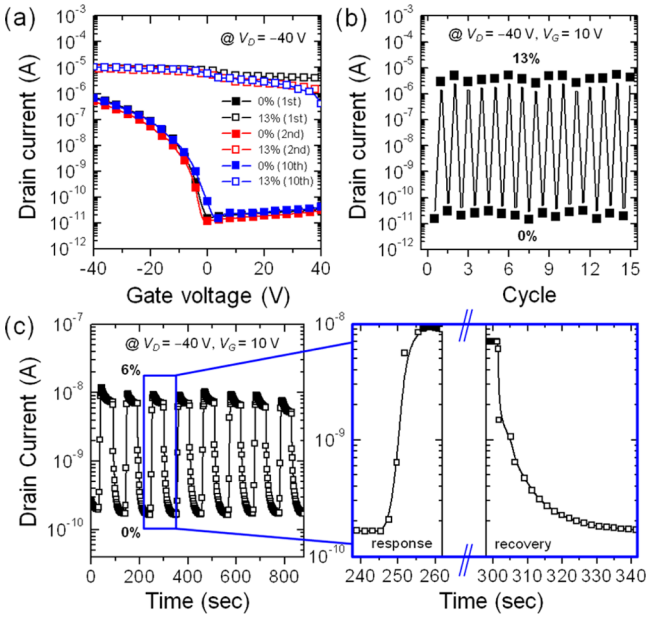

Figure 2. (a) Transfer characteristics at humidity levels that alternated between 0 and 13% (V_D = −40 V). (b) Plot of I_D at V_G = 10 V and V_D = −40 V as a function of the switching cycle. (c) Dynamic response of the current level at V_D = −40 V and V_G = 10 V upon switching the humidity levels between 0 and 6% relative humidity.

pentacene FETs containing an inserted polyelectrolyte layer during a repeated conditions sensing test in which the relative humidity level was alternated between 0 and 13%. Figure 2b summarizes the current levels collected at V_G = 10 V during 15 cycles involving switching the humidity levels. The excellent agreement between the transfer characteristics and the current levels after multiple cycles of exposure to high or low moisture levels demonstrates that the sensors displayed highly reliable performances. The sensing dynamics were examined next. Figure 2c shows a series of current levels measured for the sensor at V_G = 10 V and V_D = −40 V under sensing test conditions in which the measurement chamber environment was alternated between dry N_2 and humid N_2 (with a relative humidity of ∼6%). The current levels under the wet and dry N_2 conditions differed by 2 orders of magnitude. The transitions between levels occurred within 10 s upon exposure to wet N_2 and within 40 s upon exposure to dry N_2 (see the magnified graphs in Figure 2c). The humidity response of this sensor was

dx.doi.org/10.1021/am402050p | ACS Appl. Mater. Interfaces 2013, 5, 8591−8596

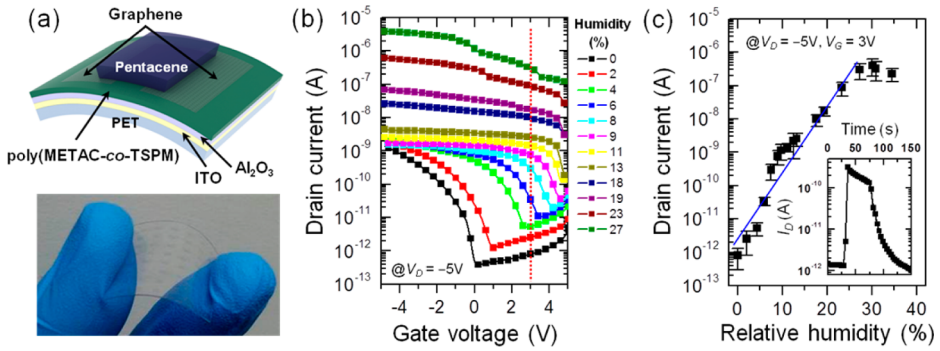

Figure 3. (a) Schematic diagram of a device and a photograph of the flexible humidity sensor. (b) Transfer characteristics at various humidity levels (V_D = −5 V). (c) Plot of I_D at V_G = 3 V and V_D = −5 V as a function of the humidity level. The inset shows the dynamic response of the flexible sensor upon exposure to a wet environment (6% relative humidity).

much faster than the response of other organic FET-type humidity sensors, which are usually responsive on the order of tens of minutes.[24,30]

Finally, we assembled humidity sensors on a flexible substrate. Here, a high-*k* Al_2O_3 layer, rather than a SiO_2 layer, was used to achieve low-voltage sensor operation. Graphene source/drain electrodes and an indium tin oxide (ITO) gate electrode were employed to take advantage of the optical transparency of these materials (Figure 3a).[8] During fabrication, a photoresist was intentionally applied onto the Al_2O_3 surface and then removed to promote surface roughness and partial dewetting of the polyelectrolyte. Despite the formation of pentacene films with poor crystallinity (Supporting Information Figure S3) after such a treatment,[38] the consequent reduction in the current levels, especially at the low humidity levels, helped enhance the current ratio between the low- and high-humidity conditions. Moreover, utilizing the partially dewetted polyelectrolyte allowed impeding the diffusion of chlorine ions within the interlayer. This resulted in the critical chlorine ion concentration yielding the saturated behavior in the drain current to be reached at higher humidity levels and thereby extension of the sensing window.

Figure 3b displays the transfer characteristics (V_D = −5 V) of the flexible pentacene humidity sensors containing an inserted polyelectrolyte interlayer under various relative humidity levels between 0 and 30%. The low operation voltage below 5 V confirmed the utility of employing a high-*k* Al_2O_3 layer.[11] Both the current levels and the threshold voltage increased with increasing humidity. The current signal changed by as much as 6 orders of magnitude as the relative humidity was varied from 0 to 30% (Figure 3c). An inflection point in the transfer characteristics, accompanied by an abrupt increase in the gate current, was also observed at low finite humidity levels (Supporting Information Figure S4). The response/recovery behavior was remarkably rapid (see the inset of Figure 3c), and the devices operated consistently during repeated cycles of exposures to humidity (Supporting Information Figure S5). Note that the current level increased continuously up to a relative humidity level of 30%, yielding a sensing window that was twice as wide as that of sensors prepared on Si/SiO_2 substrates.

CONCLUSION

In summary, we demonstrate the preparation of flexible, low-voltage, transparent pentacene humidity sensors with ultrahigh sensitivity, good reliability, and fast response/recovery behavior derived from an inserted polyelectrolyte (poly(METAC-*co*-TSPM)) interlayer. The excellent performances of these devices relies on the presence of Cl^- ions in the electrolyte dielectric layer, which were freely released under humid conditions and boosted the electrical current in the transistor channel. The introduction of a gate electrolyte layer that can trigger an electrochemical doping process in a semiconductor provides a new approach to achieving highly sensitive, flexible, and lightweight sensors, even beyond humidity sensors.

ASSOCIATED CONTENT

Supporting Information

Current−voltage characteristics of FET sensors and AFM images. This material is available free of charge via the Internet at http://pubs.acs.org.

AUTHOR INFORMATION

Corresponding Authors

*E-mail: mskang@ssu.ac.kr (M.S.K.).
*E-mail: jhcho94@skku.edu (J.H.C.).

Author Contributions

#Prof. Y. D. Park and B. Kang contributed equally to this work.

Notes

The authors declare no competing financial interest.

ACKNOWLEDGMENTS

This work was supported by a grant from the Center for Advanced Soft Electronics (CASE) under the Global Frontier Research Program (2011-0031628) and Basic Science Research Program (2009-0083540, 2012011603, and 012R1A1A1004279) of the National Research Foundation of Korea (NRF) funded by the Ministry of Education, Science and Technology, Korea.

REFERENCES

(1) Kim, D.-H.; Lu, N.; Ghaffari, R.; Kim, Y.-S.; Lee, S. P.; Xu, L.; Wu, J.; Kim, R.-H.; Song, J.; Liu, Z. *Nat. Mater.* **2011**, *10*, 316−323.
(2) Mannsfeld, S. C.; Tee, B. C.; Stoltenberg, R. M.; Chen, C. V. H.; Barman, S.; Muir, B. V.; Sokolov, A. N.; Reese, C.; Bao, Z. *Nat. Mater.* **2010**, *9*, 859−864.
(3) Someya, T.; Sekitani, T.; Iba, S.; Kato, Y.; Kawaguchi, H.; Sakurai, T. *Proc. Natl. Acad. Sci. USA* **2004**, *101*, 9966−9970.
(4) Street, R. A.; Wong, W.; Ready, S.; Chabinyc, M.; Arias, A.; Limb, S.; Salleo, A.; Lujan, R. *Mater. Today* **2006**, *9*, 32−37.
(5) Cho, J. H.; Lee, J.; Xia, Y.; Kim, B.; He, Y.; Renn, M. J.; Lodge, T. P.; Frisbie, C. D. *Nat. Mater.* **2008**, *7*, 900−906.

(6) Briseno, A. L.; Tseng, R. J.; Ling, M. M.; Falcao, E. H.; Yang, Y.; Wudl, F.; Bao, Z. *Adv. Mater.* **2006**, *18*, 2320−2324.
(7) Facchetti, A. *Chem. Mater.* **2010**, *23*, 733−758.
(8) Han, T.-H.; Lee, Y.; Choi, M.-R.; Woo, S.-H.; Bae, S.-H.; Hong, B. H.; Ahn, J.-H.; Lee, T.-W. *Nat. Photonics* **2012**, *6*, 105−110.
(9) Kang, B.; Lee, W. H.; Cho, K. *ACS Appl. Mater. Interfaces* **2013**, *5*, 2302−2315.
(10) Herlogsson, L.; Cölle, M.; Tierney, S.; Crispin, X.; Berggren, M. *Adv. Mater.* **2010**, *22*, 72−76.
(11) Sekitani, T.; Yokota, T.; Zschieschang, U.; Klauk, H.; Bauer, S.; Takeuchi, K.; Takamiya, M.; Sakurai, T.; Someya, T. *Science* **2009**, *326*, 1516−1519.
(12) Chen, Z.; Lu, C. *Sens. Lett.* **2005**, *3*, 274−295.
(13) Konvalina, G.; Haick, H. *ACS Appl. Mater. Interfaces* **2012**, *4*, 317−325.
(14) Zilberman, Y.; Ionescu, R.; Feng, X. L.; Mullen, K.; Haick, H. *ACS Nano* **2011**, *5*, 6743−6753.
(15) Liang, J.; Chen, B. Q.; Long, Y. T. *Analyst* **2011**, *136*, 4053−4058.
(16) Su, P.-G.; Wang, C.-P. *Sens. Actuators, B* **2008**, *129*, 538−543.
(17) Li, Z.; Zhang, H.; Zheng, W.; Wang, W.; Huang, H.; Wang, C.; MacDiarmid, A. G.; Wei, Y. *J. Am. Chem. Soc.* **2008**, *130*, 5036−5037.
(18) Kuang, Q.; Lao, C.; Wang, Z. L.; Xie, Z.; Zheng, L. *J. Am. Chem. Soc.* **2007**, *129*, 6070−6071.
(19) Bradley, K.; Cumings, J.; Star, A.; Gabriel, J.-C. P.; Grüner, G. *Nano Lett.* **2003**, *3*, 639−641.
(20) Bachar, N.; Mintz, L.; Zilberman, Y.; Ionescu, R.; Feng, X. L.; Mullen, K.; Haick, H. *ACS Appl. Mater. Interfaces* **2012**, *4*, 4960−4965.
(21) Wang, P.; Zhang, L.; Xia, Y.; Tong, L.; Xu, X.; Ying, Y. *Nano Lett.* **2012**, *12*, 3145−3150.
(22) Someya, T.; Dodabalapur, A.; Huang, J.; See, K. C.; Katz, H. E. *Adv. Mater.* **2010**, *22*, 3799−3811.
(23) Lin, P.; Yan, F. *Adv. Mater.* **2012**, *24*, 34−51.
(24) Zhu, Z.-T.; Mason, J. T.; Dieckmann, R.; Malliaras, G. G. *Appl. Phys. Lett.* **2002**, *81*, 4643−4645.
(25) Li, D.; Borkent, E.-J.; Nortrup, R.; Moon, H.; Katz, H.; Bao, Z. *Appl. Phys. Lett.* **2005**, *86*, 042105−042107.
(26) Braga, D.; Horowitz, G. *Adv. Mater.* **2009**, *21*, 1473−1486.
(27) Lee, C.-W.; Choi, B.-K.; Gong, M.-S. *Analyst* **2004**, *129*, 651−656.
(28) Yao, Z. W.; Yang, M. J. *Sens. Actuators, B* **2006**, *117*, 93−98.
(29) Lee, C. H.; Lim, H. S.; Kim, J.; Cho, J. H. *ACS Nano* **2011**, *5*, 7397−7403.
(30) Mahadeva, S. K.; Yun, S.; Kim, J. *Sens. Actuators, A* **2011**, *165*, 194−199.
(31) Kang, M. S.; Sahu, A.; Frisbie, C. D.; Norris, D. J. *Adv. Mater.* **2013**, *25*, 725−731.
(32) Soeda, J.; Hirose, Y.; Yamagishi, M.; Nakao, A.; Uemura, T.; Nakayama, K.; Uno, M.; Nakazawa, Y.; Takimiya, K.; Takeya, J. *Adv. Mater.* **2011**, *23*, 3309−3314.
(33) Kobayashi, S.; Nishikawa, T.; Takenobu, T.; Mori, S.; Shimoda, T.; Mitani, T.; Shimotani, H.; Yoshimoto, N.; Ogawa, S.; Iwasa, Y. *Nat. Mater.* **2004**, *3*, 317−322.
(34) Lee, J.; Kaake, L. G.; Cho, J. H.; Zhu, X.-Y.; Lodge, T. P.; Frisbie, C. D. *J. Phys. Chem. C* **2009**, *113*, 8972−8981.
(35) Cho, J. H.; Lee, J.; He, Y.; Kim, B.; Lodge, T. P.; Frisbie, C. D. *Adv. Mater.* **2008**, *20*, 686−690.
(36) Panzer, M. J.; Frisbie, C. D. *J. Am. Chem. Soc.* **2007**, *129*, 6599−6607.
(37) Dodgen, H.; Jordan, A.; Jordan, R. *J. Phys. Chem.* **1973**, *77*, 2149−2153.
(38) Yoon, M.-H.; Kim, C.; Facchetti, A.; Marks, T. J. *J. Am. Chem. Soc.* **2006**, *128*, 12851−12869.